HOSTED BY

ELSEVIER

Available online at www.sciencedirect.com

ScienceDirect

Soils and Foundations xxx (xxxx) xxx

SOILS AND FOUNDATIONS

www.elsevier.com/locate/sandf

Technical Note

A new abrasive wear model for railway ballast

John de Bono, Huiqi Li *, Glenn McDowell

University of Nottingham, United Kingdom

Received 4 October 2019; received in revised form 17 April 2020; accepted 8 May 2020

Abstract

A new method to model the abrasion of granular particles using the discrete element method is demonstrated in this paper. This new, simple method is based on a classical theory of abrasive wear, relating the volume of solid lost to the frictional work at particle contacts. The modelling technique is demonstrated in simulations of railway ballast using realistically-shaped particles, which are compared to experimental data. The new abrasion model correctly introduces stress-dependent behaviour at small strains into the simulations, which is essential for any realistic discrete element model.

Keywords: Discrete element method; DEM; Abrasion; Wear; Ballast; Damage; Degradation; Triaxial

1. Introduction

Abrasion of railway ballast is a major contributor to track degradation (McDowell et al., 2005; Abadi et al., 2018). Abrasive wear of ballast particles reduces the ballast shear strength, leading to increased strains; and contributes to ballast fouling, which reduces drainage capacity. A significant proportion of the costs of ballast maintenance can therefore be attributed to abrasion.

Abrasive wear, or simply abrasion, is used here to broadly refer to the permanent wear or damage caused to ballast particles by grinding or sliding against one another under load. Due to the large size of ballast particles, relatively narrow gradation, and very large loads from traffic, large contact forces occur between ballast particles which inevitably lead to abrasion. Abrasion typically manifests itself as a loss of angularity, producing more rounded particles, and should be considered distinct from particle breakage or splitting.

Abrasion has long been known acknowledged (and is one reason why granite ballast is preferred over limestone), however the phenomenon has rarely been quantified. This short paper seeks to investigate the effects of ballast particle abrasion on simple discrete element method (DEM) simulations by implementing a very simple abrasion mechanism, accompanied by data from experimental triaxial tests on real ballast.

2. Ballast wear

2.1. Experimental

Ballast abrasion has been frequently observed experimentally. Brown et al. (2007) and Abadi et al. (2018) for example both used painted ballast particles to highlight any surface damage and enable an easy visual comparison of particles before and after loading. Brown et al. subjected a large-scale bed of ballast to cyclic loading from three sleepers. The ballast bed contained vertical columns of painted particles, located in positions anticipated to experience the greatest damage. Visual inspection revealed obvious rounding-off of the corners, although this study had a

Peer review under responsibility of The Japanese Geotechnical Society.

* Corresponding author.
E-mail address: Huiqi.Li@nottingham.ac.uk (H. Li).

https://doi.org/10.1016/j.sandf.2020.05.001

Please cite this article as: J. de Bono, H. Li and G. McDowell, A new abrasive wear model for railway ballast, Soils and Foundations, https://doi.org/10.1016/j.sandf.2020.05.001

particular focus on the effects of tamping. Similarly, Abadi et al. (2018) performed tests on a bed of particles loaded cyclically by a single sleeper, with painted particles distributed across the top of the bed underneath the sleeper. Weighing the selected particles before and after revealed losses of mass in the range 0.1–0.3% after several million cycles. Other studies such as those by Indraratna et al. (2005) and Lackenby et al. (2007) have also commented on the evidence of abrasion and surface damage to particles.

The large triaxial apparatus at the University of Nottingham has been used for a number of years to shear full-size railway ballast (e.g. Aursudkij, McDowell and Collop, 2009). A typical sample of ballast in this apparatus, prepared with a grading satisfying UK rail standards, contains around 600–1000 particles. At most confining pressures (30–90 kPa), visual inspection of samples after testing reveals very few obviously broken (split) particles, similar to what has been reported by Indraratna et al. (2005). However, the fact that the peak shear strength and amount of dilation both reduce with increasing confining pressure, strongly suggests that some form of particle damage occurs, implying that less obvious damage may occur such as abrasion and/or breakage of asperities. Anecdotal evidence obtained by the authors from weighing samples before and after triaxial testing suggests that approximately up to 0.5% of the total mass is lost to abrasion at confining pressures in the region 30–90 kPa, but this is difficult to reliably quantify, and likely also includes abrasion resulting from sample preparation and compaction. Photographs of ballast particles before and after being subjected to abrasive damage are shown in Fig. 1.

2.2. Theoretical

Classical theories for abrasive wear relate the volume of mass lost due to abrasion to the frictional work (e.g. Archard, 1953) between two materials. This is commonly expressed in the form:

$$V \sim F_N S \tag{1}$$

where V is the loss of volume, F_N is the normal contact force, and S is the sliding distance. The proportionality in Eq. (1) is a function of the material properties, and is often termed the wear coefficient or specific wear rate. Attempts to implement abrasion into geotechnical DEM models most often involve breakable asperities (e.g. Lu and McDowell, 2006; McDowell and Li, 2016), or changing contact properties, such as making the coefficient of friction a function of contact force (e.g. Harkness et al., 2016). In this work, a very simple implementation of abrasion based on Eq. (1) is demonstrated and used in simulations of triaxial tests. Similar (i.e. using DEM) but unrelated attempts to simulate material wear using Eq. (1) include Ning and Ghadiri (2006) and Rojek (2014).

3. DEM model

The triaxial tests presented here feature a cylindrical sample 450 mm in height by 300 mm diameter, enclosed by a flexible lateral membrane and two rigid platens. The triaxial tests are performed by applying strain increments to the upper platen, as is the case in the real tests, whilst maintaining a constant confining pressure and allowing free radial deformation. The membrane consists of 4320 triangular facets, and the confining pressure is applied via a servo-function which moves the vertices independently to ensure a uniform applied stress. Further details of this model and images of the membrane may be found in de Bono and McDowell (2018). In the simulations, the initial stage of the tests are stress-controlled (following Coop, 1990), to allow better observations of the stiffness during the early stages. The particles modelled, shown in Fig. 2, are based on real ballast particles. A surface was generated from a 3D scan (a), which was then used to form a DEM particle constructed out of spheres (b). In the triaxial simulations, only a single shape of particle was used, but with a distribution of sizes. Each particle has a uniform density,

Fig. 1. Images of ballast particles subjected to wear: before (a) and after (b).

Please cite this article as: J. de Bono, H. Li and G. McDowell, A new abrasive wear model for railway ballast, Soils and Foundations, https://doi.org/10.1016/j.sandf.2020.05.001

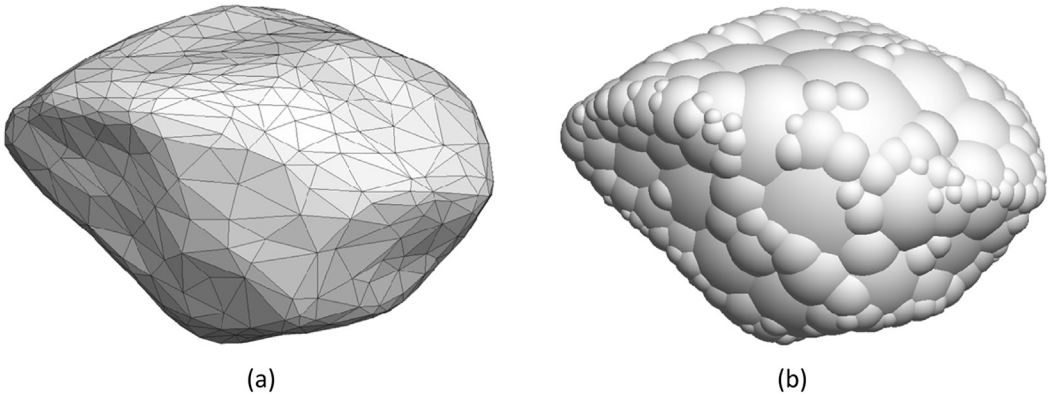

Fig. 2. Simulated ballast particle. Surface scan (a), virtual particle made of spheres (b).

and is formed of around 200 spheres, which overlap but do not physically interact with each other. An example sample is shown in Fig. 3, which adheres to UK guidelines for ballast gradation (EN 1345, 2013). The Hertz contact model (Itasca, 2015) is used with a shear modulus of 28 GPa, a typical value for quartz-like particles (Ashby and Jones, 1986), and the coefficient of friction is set (arbitrarily) to 0.5. As the simulations are quasi-static and confined, mechanical damping is used with a damping coefficient of 0.7 (Itasca, 2015), which allows the simulations to achieve equilibrium efficiently. Provided reasonably high contact stiffnesses are used, the choice of contact model and actual stiffness has no effect on the abrasion method (only if extremely low contact stiffnesses were used would there be an affect, due to large overlaps and greater coordination numbers). The abrasion model is however sensitive to the damping method. Using a much lower damping coefficient (or none) would result in excessive kinetic energy and particle oscillations. Without using mechanical damping (for example if simulating dynamic tests), an alternative means of reducing kinetic energy would be required such as collision-based viscous damping or some form of drag. Nonetheless, all simulations here have the exact same properties.

To allow abrasion, frictional work is accumulated at each individual contact. For a single contact between two ballast particles, the frictional work W accumulated in a single timestep is given by:

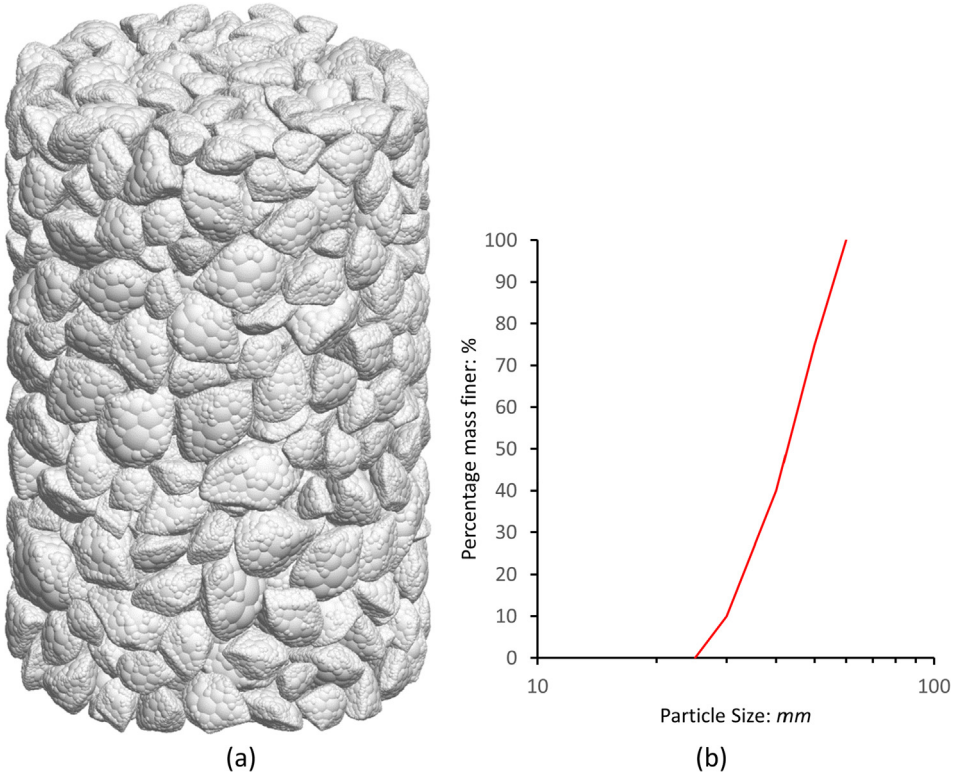

Fig. 3. Virtual DEM triaxial sample (a) and particle size distribution (b).

Please cite this article as: J. de Bono, H. Li and G. McDowell, A new abrasive wear model for railway ballast, Soils and Foundations, https://doi.org/10.1016/j.sandf.2020.05.001

$$W = F_S S \quad (2)$$

where F_S is the average shear force during the timestep, and S is the sliding displacement (the total shear displacement at a contact may include both elastic and sliding components). If sliding is occurring, then the shear force $F_S = \mu F_N$, where μ is the coefficient of friction, which is consistent with Eq. (1). Assuming the volume of solids lost due to abrasion is proportional to the frictional work (Archard, 1953), choosing a suitable coefficient of proportionality k allows the volume of solid lost to be calculated as:

$$\Delta V = k\mu F_N S \quad (3)$$

To facilitate this loss of volume, ΔV, the individual spheres in any ballast particle may gradually shrink (flatten), reducing the overall angularity of the ballast particle. The DEM procedure for abrasion is summarised as follows: for any given contact, the loss of volume is calculated using Eqs. (1) and (2) and a given coefficient of proportionality. For simplicity, this volume loss is apportioned equally to the two individual spheres that are in contact with each other (in different ballast particles). The loss of volume is realised by causing each subsidiary sphere to recede into the 'parent' ballast particle. This is performed in a way so that the surface area of the larger sphere which is covered by the smaller sphere does not change as the smaller sphere recedes. This is implemented by moving the smaller sphere inwards, towards the centroid of the nearest and largest overlapping sphere, whilst simultaneously expanding its radius. A simple diagram illustrating this method in 2D is given in Fig. 4. This method means that the protrusion of any individual sphere gradually diminishes and becomes flatter with abrasion. In nearly all cases, each individual sphere overlaps several other spheres, so an exact calculation of how much to move any sphere in order to achieve the desired nett loss of volume of the overall ballast particle is non-trivial. Therefore, an initial estimate is made of how much to recede the sphere, then a voxelization method is used to achieve the correct result. The voxelization method divides a small enclosing volume into finite small cubes, and sums all the cubes whose centroid lies within a sphere belonging to the ballast particle. Due to the relatively small amount of abrasion and quasi-static nature of these tests, the lost dust is not considered to be of significant mechanical importance in these initial simulations, and is therefore not accounted for. However, this is a simplification for convenience; for weaker materials at large strains or any other scenarios in which the dust may be mechanically (or hydraulically) important, it would be inaccurate to neglect the loss of mass.

4. Results

4.1. Experimental

Typical experimental triaxial results for real ballast are shown in Fig. 5, obtained from conventional drained tests at confining pressures of 30, 60 and 90 kPa. Due to the size of the sample and constraints of the apparatus, it is not possible to reach large axial shear strains and/or critical states. As such, at the end of the tests all three show continuing dilation, and it can be assumed that continuing the tests to further strains would allow all samples to undergo strain softening and eventually reach steady states.

Fig. 5(a) shows the stress ratio ($=q/p$) responses of the 3 samples of ballast sheared at the different confining pressures. Despite the fact that steady or critical states aren't reached, the 3 tests exhibit different peak stress ratios, meaning the peak envelope in q-p space is curved and implying stress-dependent behaviour (i.e. particle damage). Visual inspection of the samples after testing, both in general and for these 3 specific tests, reveals limited evidence of major particle splitting/breakage, which appears insensitive to the confining pressure. However, the higher confining pressure tests (in this case 90 kPa), in general do visually reveal a moderately higher degree of minor damage, such as the chipping of corners. Fig. 5(b) shows how increasing the confining pressure suppresses the dilation, as one would expect, which is also attributable to the particle damage that occurs.

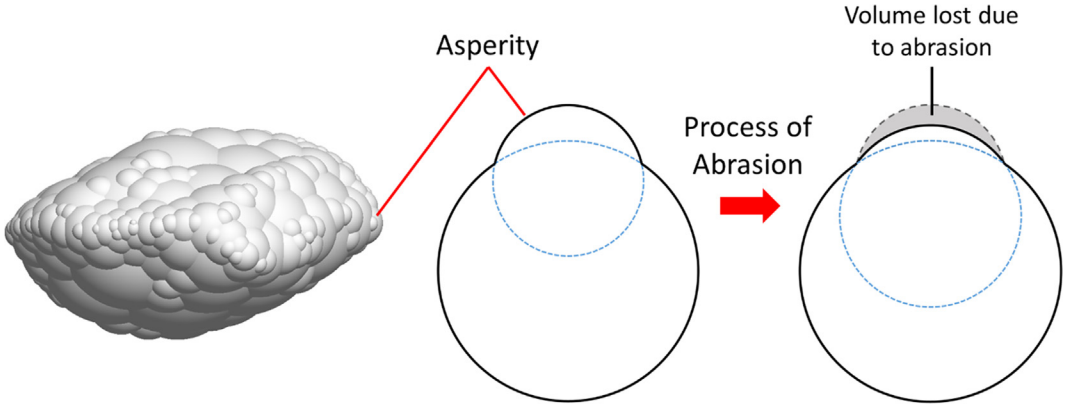

Fig. 4. Method of abrasion used in DEM.

Please cite this article as: J. de Bono, H. Li and G. McDowell, A new abrasive wear model for railway ballast, Soils and Foundations, https://doi.org/10.1016/j.sandf.2020.05.001

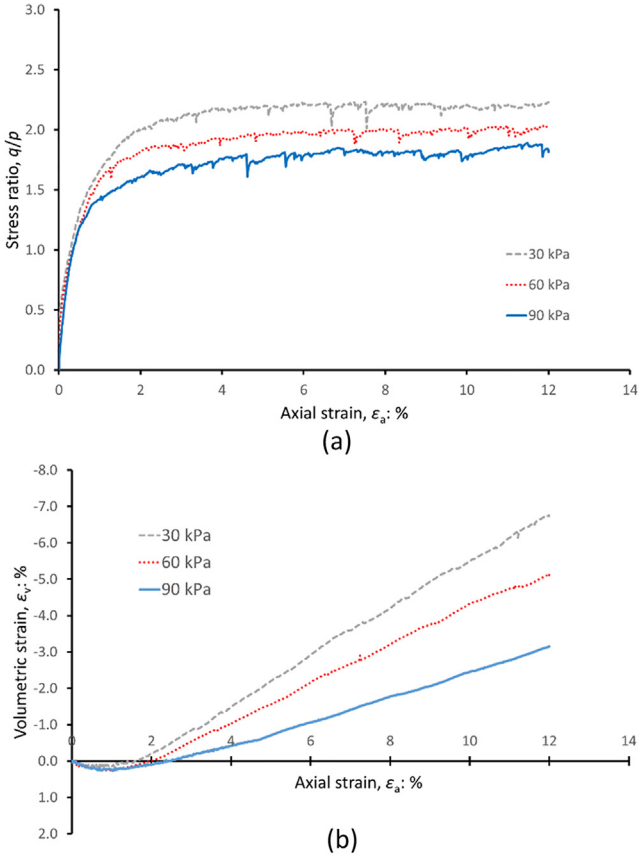

Fig. 5. Experimental triaxial test results on real ballast: shear stress (a) and volumetric behaviour (b).

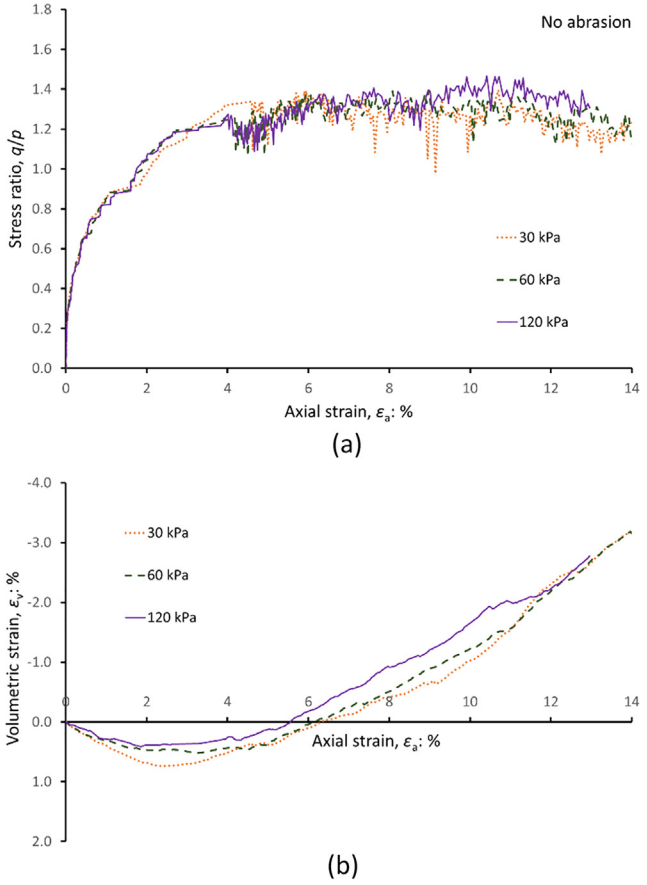

Fig. 6. DEM triaxial results with no abrasion: stress ratio (a) and volumetric strain (b).

4.2. DEM

Triaxial results from simulations in which no abrasion occurs are shown in Fig. 6, which provide a base comparison for the subsequent simulations featuring abrasive degradation. The first observation is that both the stress ratio and volumetric responses appear approximately the same, with no effect from the confining pressure. This has been shown before in DEM simulations in which no particle damage occurs (e.g. de Bono and McDowell, 2014).

For each set of DEM results shown here, a single sample is used. That is, Figs. 6–8 are each based on a single initial sample. Explicitly, that means a single sample is isotropically compressed to 30, 60 and then 120 kPa. Separate triaxial tests are performed (in parallel) from each of these stresses. So although the triaxial tests are based on the same sample, they have been confined to different stresses and therefore the tests at the larger stresses have slightly greater densities and have experienced slightly more abrasion. The use of the same samples for each set of tests provides a more controlled comparison for each case compared to real experiments which would require a new—and statistically different—sample for each triaxial test.

Fig. 7 shows equivalent plots for simulations including abrasion. The loss of volume at all contacts is calculated using Eq. (3) with a wear rate of $k = 10^{-8}$ m^2/N, which was chosen arbitrarily as a conservative first estimate. Comparing the results with Fig. 6 shows that the inclusion of abrasion introduces stress-dependent behaviour. The shear stress responses still appear largely similar between the 3 tests, however at low strains (e.g. $\varepsilon_a < 4\%$) the materials display slightly different stress ratio responses. Increasing the confining pressure gives the appearance of decreasing the initial stiffness of the material, causing the stress ratio curve to become slightly 'flatter'. This trend, which was absent in the simulations without abrasion, is consistent with the real ballast behaviour (Fig. 5), and is commonly observed for all granular materials (e.g. Yamamuro and Lade, 1996). The three materials in Fig. 7 also exhibit less dilation, which becomes supressed by increasing confining pressure, which in turn increases abrasion.

Although the inclusion of abrasion may affect the peak stress ratio (or friction angle), it should have no effect on the material's critical state friction angle, which is a function of inter-particle friction and particle shape. Although critical states were not reached in these simulations, the data in Fig. 7 supports a single critical state stress ratio independent of confining pressure. Points of minimum volume in the volumetric responses are often assumed to

Please cite this article as: J. de Bono, H. Li and G. McDowell, A new abrasive wear model for railway ballast, Soils and Foundations, https://doi.org/10.1016/j.sandf.2020.05.001

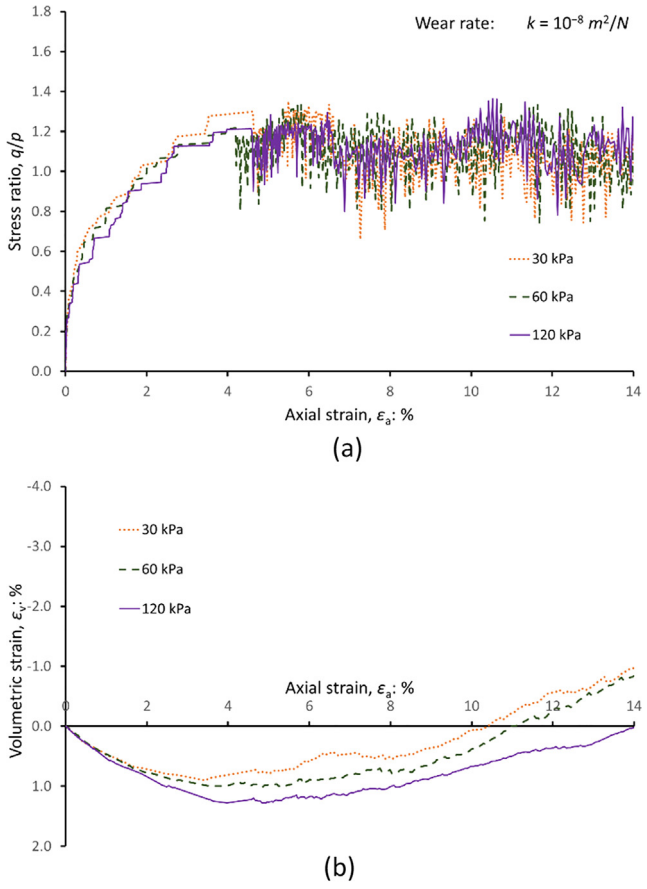

Fig. 7. DEM triaxial results from simulations including abrasion: stress ratio (a) and volumetric strain (b).

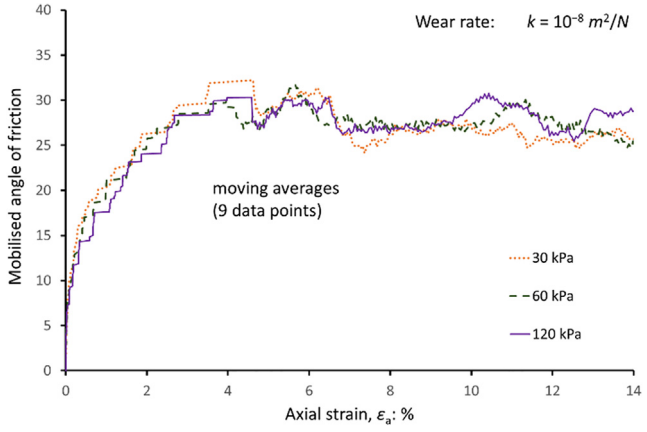

Fig. 8. Mobilised friction as a function of axial strain using a moving average technique.

correspond to the critical state stress ratio. The point of minimum volume (and zero volume change) at 30 kPa occurs at around 3.5% axial strain, and at around 4% axial strain in the 60 kPa and 120 kPa tests. In all three tests, these points correspond to a stress ratio of 1.2. The dilative behaviour begins at greater axial strains in the simulations compared to the experimental data; the real triaxial sample is clearly stiffer. This is a result of the simplified particle shape used in the simulations. Although more realistic than using spheres, the simulated particles are still less angular. It could be possible to compensate for this by implementing an artificially high coefficient of friction or implementing some form of rolling-resistance between the particles, however the aim of this paper was not to adjust input parameters in order to achieve an exact calibration, but rather to capture the general correct stress-dependent behaviour caused by abrasion.

It is clear that introducing (and as will be shown, increasing) the rate of abrasion increases the amount of fluctuations visible in the stress–strain plots. This is due to the method of modelling abrasion: when a sphere is receded, this causes a total removal of the ballast-to-ballast contact, which would have been transferring a force as part of a contact force chain. This inevitably causes a reduction in the measured macroscopic axial stress (which is not as visible in experimental data where this process occurs on a much more gradual and finer scale). To give a clearer idea of the trend in these simulations, the mobilised friction is plotted in Fig. 8 but using a moving average technique (±4 neighbouring data points) to suppress the fluctuations.

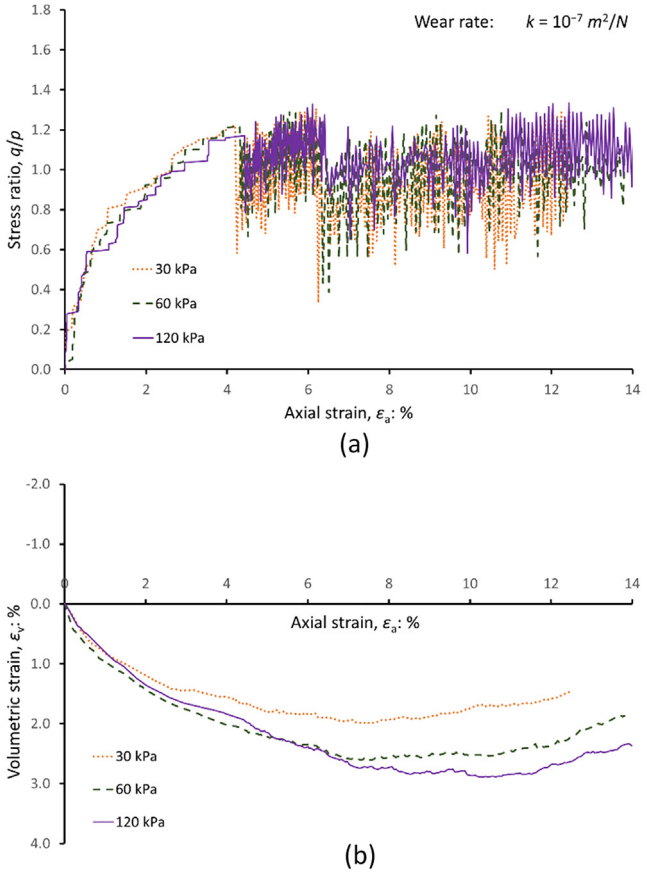

Fig. 9. DEM results with increased abrasion: stress ratio (a) and volumetric strain (b).

Please cite this article as: J. de Bono, H. Li and G. McDowell, A new abrasive wear model for railway ballast, Soils and Foundations, https://doi.org/10.1016/j.sandf.2020.05.001

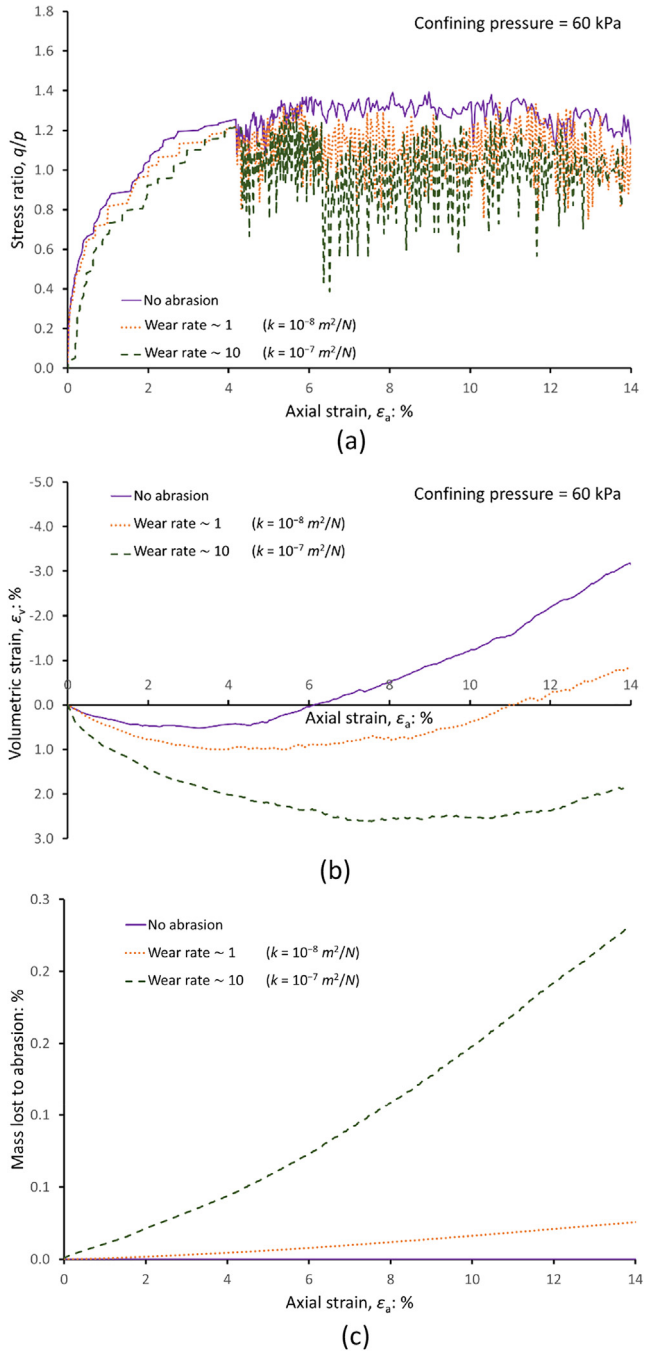

Fig. 10. DEM triaxial results showing effects of rate of abrasion. Stress ratio (a), volumetric strain (b), lost mass (c).

It is worth noting that in Fig. 7 (and to a greater extent in Fig. 9), the tests at lower confining pressures exhibit larger momentary drops in stress ratio, and therefore larger fluctuations. This may give the (potentially misleading) impression that the tests at lower confining pressures demonstrate a slightly lower ultimate shear strength—which may also be interpreted from Fig. 8. However, in all cases, the fluctuations—or more specifically the sudden temporary losses in shear stress in Figs. 7 and 9—are rapidly recovered, and it is postulated that for this particular study, it may be acceptable to only consider the peak values (i.e., connecting the peaks and discarding the troughs). The larger fluctuations in stress ratio are a result of the difference in stress levels between the tests (e.g. $\sigma_3 = 120$ vs 30 kPa).

Fig. 9 shows similar simulation results but with a 10 times greater wear coefficient ($k = 10^{-7}$ m^2/N). The stress ratio responses are similar to Fig. 7, with the confining pressure mainly affecting the initial gradient of the stress ratio curve. The most notable difference however is in the volumetric behaviour, with all 3 samples displaying greatly delayed and reduced dilatancy.

Fig. 10 compares results with the 2 different wear rates and no abrasion at all, at a confining pressure of 60 kPa. It can be seen here that increasing the rate of abrasion causes the stress ratio curves to become flatter, and reduces the peak stress ratio and dilatancy. The most striking observation is the difference in volumetric behaviour, which appears more extreme than the changes in stress ratio response. Fig. 10(c) shows the cumulative mass lost throughout these 3 tests. The test with the higher wear coefficient loses approximately 10 times more mass compared to the lower wear rate, however the total mass lost still appears small at less than 0.5%, showing just how significant abrasion is with regard to the macroscopic response.

5. Conclusions

A very simple method for implement particle abrasion has been implemented into DEM models of triaxial tests on railway ballast. Despite its simplicity, this method has been shown to introduce stress-dependent behaviour, namely a flattening of the stress ratio response at low strains, a reduction in peak strength, and a suppression of dilatancy with increasing confining pressure and/or abrasion. All of these well-known aspects of behaviour are absent in numerical models which do not account for particle degradation. This study has demonstrated a simple approach to account for abrasion in DEM models, and also reveals just how significantly an ostensibly small amount of abrasion can influence the observed macroscopic behaviour, which should no longer be simply ignored in DEM models. Of key importance is the fact that the simple wear model only affects the interlock/dilation, and not the overall form of the particle, and hence this work would suggest that the critical state is unaffected by the abrasive wear of particles.

Acknowledgements

This work was supported by the Engineering and Physical Sciences Research Council [grant number EP/M025276/1].

Please cite this article as: J. de Bono, H. Li and G. McDowell, A new abrasive wear model for railway ballast, Soils and Foundations, https://doi.org/10.1016/j.sandf.2020.05.001

References

Abadi, T. et al., 2018. Improving the performance of railway tracks through ballast interventions. Proc. Inst. Mech. Eng., Part F: J. Rail Rapid Transit 232 (2), 337–355. https://doi.org/10.1177/0954409716671545.

Archard, J.F., 1953. Contact and Rubbing of Flat Surfaces. J. Appl. Phys. 24 (8), 981–988. https://doi.org/10.1063/1.1721448.

Ashby, M.F., Jones, D.R., 1986. Engineering Materials 2: An Introduction to Microstructures, Processing and Design. Pergamon Press, New York.

Aursudkij, B., McDowell, G.R., Collop, A.C., 2009. Cyclic loading of railway ballast under triaxial conditions and in a railway test facility. Granular Matter 11 (6), 391–401. https://doi.org/10.1007/s10035-009-0144-4.

de Bono, J.P., McDowell, G.R., 2014. DEM of triaxial tests on crushable sand. Granular Matter 16 (4), 551–562. https://doi.org/10.1007/s10035-014-0500-x.

de Bono, J.P., McDowell, G.R., 2018. Micro mechanics of drained and undrained shearing of compacted and overconsolidated crushable sand. Géotechnique 68 (7), 575–589. https://doi.org/10.1680/jgeot.16.P.318.

Brown, S.F., Brodrick, B.V., Thom, N.H., McDowell, G.R., 2007. The Nottingham railway test facility, UK. Proc. Inst. Civil Eng. – Transport 160 (2), 59–65. https://doi.org/10.1680/tran.2007.160.2.59.

Coop, M.R., 1990. The mechanics of uncemented carbonate sands. Géotechnique 40 (4), 607–626. https://doi.org/10.1680/geot.1990.40.4.607.

EN 13450, B., 2013. Aggregates for railway ballast. British Standards Institution.

Harkness, J. et al., 2016. 'Discrete element simulation of railway ballast: modelling cell pressure effects in triaxial tests', *Granular Matter*. Springer, Berlin Heidelberg, p. 65, http://doi.org/10.1007/s10035-016-0660-y.

Indraratna, B., Lackenby, J., Christie, D., 2005. Effect of confining pressure on the degradation of ballast under cyclic loading. Géotechnique 55 (4), 325–328. https://doi.org/10.1680/geot.55.4.325.65490.

Itasca, 2015. 'PFC3D'. Itasca Consulting. Group Inc..

Lackenby, J. et al., 2007. Effect of confining pressure on ballast degradation and deformation under cyclic triaxial loading. Géotechnique 57 (6), 527–536. https://doi.org/10.1680/geot.2007.57.6.527.

Lu, M., McDowell, G.R., 2006. Discrete element modelling of ballast abrasion. Géotechnique 56 (9), 651–655. https://doi.org/10.1680/geot.2006.56.9.651.

McDowell, G.R., Lim, W.L., Collop, A.C., Armitage, R., Thom, N.H., 2005. Laboratory simulation of train loading and tamping on ballast. Proc. Inst. Civil Eng. – Transport 158 (2), 89–95. https://doi.org/10.1680/tran.2005.158.2.89.

McDowell, G.R., Li, H., 2016. Discrete element modelling of scaled railway ballast under triaxial conditions. Granular Matter 18 (3), 66. https://doi.org/10.1007/s10035-016-0663-8.

Ning, Z., Ghadiri, M., 2006. Distinct element analysis of attrition of granular solids under shear deformation. Chem. Eng. Sci. 61 (18), 5991–6001. https://doi.org/10.1016/j.ces.2006.03.056.

Rojek, J., 2014. Discrete element thermomechanical modelling of rock cutting with valuation of tool wear. Comput. Particle Mech. 1 (1), 71–84. https://doi.org/10.1007/s40571-014-0008-5.

Yamamuro, J.A., Lade, P.V., 1996. Drained Sand Behavior in Axisymmetric Tests at High Pressures. J. Geotech. Eng. 122 (2), 109–119. https://doi.org/10.1061/(ASCE)0733-9410(1996)122:2(109).

Please cite this article as: J. de Bono, H. Li and G. McDowell, A new abrasive wear model for railway ballast, Soils and Foundations, https://doi.org/10.1016/j.sandf.2020.05.001